Finding neural correlates of drift diffusion processes in EEG oscillations

Marieke K. van Vugt (m.k.van.vugt@rug.nl)
Department of Artificial Intelligence, Nijenborgh 9
9747 AG Groningen, The Netherlands

Patrick Simen (psimen@math.princeton.edu) and

Jonathan D. Cohen (jdc@princeton.edu)
Princeton Neuroscience Institute, Green Hall
Princeton, NJ 08540 USA

Abstract

Recent studies have begun to elucidate the neural correlates of evidence accumulation in perceptual decision making. Few of them have used a combined modeling-electrophysiological approach to studying evidence accumulation. We introduce a novel multivariate approach to EEG analysis with which we can perform a comprehensive search for neural correlates of dynamics predicted by the drift diffusion model. We show that the dynamics of evidence accumulation are correlated with decreases in the 4–9 Hz theta band over the course of a trial. The rate of decrease in this band correlates with individual differences in fitted drift diffusion model parameters.

Keywords: EEG; drift diffusion model; decision making

Introduction

Every day we make thousands of decisions, and modeling work has attempted to describe the nature of these decision processes. With the advent of cognitive neuroscience, there has been a growing interest in its neural correlates. This paper introduces a novel approach to studying decision dynamics with human electrophysiology. By using model-predicted decision dynamics as regressors, we perform a comprehensive search for oscillatory features of electroencephalography (EEG) activity that could reflect evidence accumulation.

The presence of oscillations in EEG measurements indicates that neurons in a region have an increased level of spiking relative to their baseline (Fries, Nikolić, & Singer, 2007). Through being synchronized, the oscillations become strong enough in power to be visible on the scalp. This synchronization is thought to allow groups of neurons to communicate with each other (Fries, 2009; Womelsdorf et al., 2007). The brain also appears to use oscillations in conjunction with spikes to encode information, for example phase coding, where the phase of an oscillation at which a neuron fires encodes the spatial location of an animal (Fries et al., 2007; O'Keefe & Recce, 1993).

The most well-known oscillations are those in the 28–90 Hz gamma band, which have been studied extensively in the context of attention tasks. A prominent finding is that attention increases the amplitude of occipital 28–90 Hz gamma oscillations (e.g., Fries et al., 2007). Yet some studies have shown that also oscillations of lower frequency are important for attention. Busch and VanRullen (2010) found that stimuli are better perceived at certain phases of the on-going 4–9 Hz theta oscillation than at other phases. This has led to the idea that sustained attention is not actually sustained, but rather has an oscillating quality. Moreover, it suggests that 4–9 Hz theta oscillations, which until recently have primarily been associated with memory (Kahana, Seelig, & Madsen, 2001) and spatial navigation (e.g., O'Keefe & Burgess, 1999), are also relevant to perception.

On a more abstract level, it has been suggested that theta oscillations are crucial for the coordination of multiple sources of activity at decision points (Womelsdorf, Vinck, Leung, & Everling, 2010), and combining various pieces of evidence (van Vugt, Sekuler, Wilson, & Kahana, in revision). Theta oscillations have also been found to covary with decision certainty (Jacobs, Hwang, Curran, & Kahana, 2006) and prediction errors in decision making (Cavanagh, Frank, Klein, & Allen, 2010). This suggests that theta oscillations could in fact have a more fundamental role in decision making, namely the accumulation of evidence.

Evidence accumulation plays a fundamental role in accumulator models of decision making like the Drift Diffusion Model (DDM; Ratcliff, 1978). This model posits that to make a decision, a person accumulates information until they reach a threshold. Their response times (RTs) can be predicted by adding a fixed non-decision time to the time it takes to reach the threshold. The model has thresholds belonging to each response alternative, and reaching the correct threshold leads to a correct response. The speed with which one accumulates evidence on average is referred to as the 'drift rate' of the accumulation process. This model is capable of explaining complete RT distributions, not just average RTs like most models of cognition.

In our study, we examine the hypothesis that theta oscillations, but not oscillations at other frequencies, reflect evidence accumulation as predicted by the DDM. We will also test whether the dynamics of theta oscillations covary with DDM parameters estimated from a participant's behavioral data. This will not only further our understanding of human decision making, but may eventually allow us to distinguish different implementations of the DDM that cannot be disentangled solely based on behavioral data (Ditterich, 2010).

Methods

Task: Participants performed a perceptual decision making task in which they judged the direction of motion (left

or right) of a display of randomly moving dots of which a percentage moved to the left or the right. These random dot kinematograms were similar to those used in a series of psychophysical and decision making experiments with monkeys as participants (e.g., Britten, Shadlen, Newsome, & Movshon, 1992; Gold & Shadlen, 2001; Shadlen & Newsome, 2001). Stimuli consisted of an aperture of approximately 3 inch diameter viewed from approximately 100 cm (approximately 4 degrees visual angle) in which white dots (2 x 2 pixels) moved on a black background. A subset of dots moved coherently either to the left or to the right on each trial, whereas the remainder of dots were distractors that jumped randomly from frame to frame. Motion coherence was defined as the percentage of coherently moving dots. Dot density was 17 dots/square degree, selected such that individual dots could not easily be tracked.

We had a control task in which participants did not need to integrate evidence (non-integration condition). In this condition, each trial started with random dot motion, followed by an arrow indicating the direction to which a participant should respond. The arrow onset time was calibrated (based on RTs in previous blocks of the non-integration condition) such that the dot-motion-viewing times in these trials mirrored the response time distribution of the dots trials.

The experiment presentation code was written in PsychToolbox (Brainard, 1997). Dots were presented with PsychToolbox extensions written by J. I. Gold (`http://code.google.com/p/dotsx/`).

Participants: Twenty-three participants (12 female; 21 right-handed, mean age 25, range 18–38) participated in our experiment in exchange for payment. The experiment was approved by the Internal Review Board of Princeton University. Participants engaged in 3 separate hour-long training sessions in which they became familiar with the task. At the end of these training sessions, performance on a psychometric block was used to determine the coherences at which they performed at approximately 70 and 90% correct. These coherence levels were used for the two EEG sessions.

Recording Methods: We recorded EEG data from 128 channels using Neuroscan EEG caps with a Sensorium EPA-6 amplifier. Data were digitized at 1000 Hz and band-pass filtered from 0.02–300 Hz; all impedances < 30 kΩ. Acquisition was controlled by Cogniscan. All data were referenced to the nose or chin-electrode and off-line rereferenced to an average reference after automatic bad channel removal (Friederici, Wang, Herrmann, Maess, & Oertel, 2000; Hestvik, Maxfield, Schwartz, & Shafer, 2007).

General Linear Model for EEG

We developed a General Linear Model (GLM) method to correlate the predicted DDM dynamics with the EEG time series. For every trial, we modeled a ramp of activity starting at stimulus onset and ending at the response. We contrasted this ramp with a down-going ramp that began with a transient initial jump at stimulus onset. The sum of the up- and downramps forms a "boxcar," or step function. modeling the alternative hypothesis of a generic "task-on" state. We created a set of parallel up-ramps, down-ramps and boxcars for the arrow control task.

In addition to these, we created a set of nuisance regressors, modeling transient neural responses to stimulus onset and button press, and eye activity. To determine the canonical stimulus-locked response, we computed for every participant individually the stimulus-related average in electrode Cz and inserted this average waveform (from 0–300 ms post-stimulus) in the regressor at any timepoint where a stimulus was presented. Similarly, we used the average response-locked waveform from -200–0 ms relative to the response in CPz as the response regressor.[1] The eyeblink regressor was created from the activity of the eye channel.[2]

The regressors of interest consisted of ramps, which started at stimulus onset for each trial, and ramped up to a value of 1 at the time of the response. To test our hypotheses regarding ramping activity, we created separate ramp regressors for dots (integration) and arrows (non-integration) trials. We compared the fits of these regressors to regressors reflecting the alternative hypotheses of neural activity that is "on" during the trial ("boxcar") and neural activity that reflects a transient initial response slowly decreasing over the trial duration.

A major problem in GLM analyses of EEG data is the poor signal-to-noise ratio (SNR). To increase the SNR we created features (independent variables in the regression) that only consisted of the trials themselves, padded with 300 ms before the stimulus and after the response, pasted together into a single time series. We created features both from the raw EEG time series, and from wavelet-convolved signals in the delta (2–4 Hz), theta (4–9 Hz), alpha (9–14 Hz), beta (14–28 Hz), low gamma (28–48 Hz) and high gamma (48–90 Hz) ranges. After construction, we downsampled these features to 50 Hz, and z-transformed them.

We ran the GLM in two steps. In the first step we modeled all the nuisance regressors. The regressors of interest were then modeled on the residuals of this first regression, which ensured that the nuisance regressors could not influence the fits for the regressors of interest. In addition to computing the regression coefficients for each feature, we also computed the variance explained by correlating the feature with the fitted regressors (Tabachnick & Fidell, 2005).

Results

Before turning to the electrophysiological results, we discuss our behavioral data. Participants were engaged in a random dot motion discrimination paradigm, where the level of mo-

[1] Response-related ERP peaks typically show their maximum more posteriorly than stimulus-related ERP peaks. Cz and CPz are two central electrodes that show peak responses to stimulus presentation and button presses, respectively.

[2] We set this regressor to zero outside the eyeblink episodes detected with an amplitude threshold to ensure that no random fluctuations in the eye channel would distort our results. We focused exclusively on eyeblinks and not on horizontal eye movements because we only had a single eye electrode placed underneath the left eye.

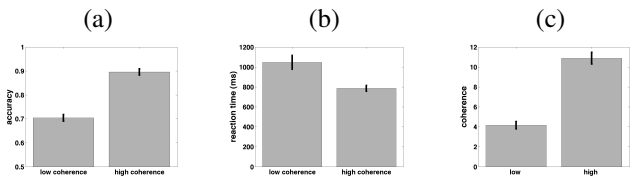

Figure 1: Mean accuracy (a), reaction time (b) and coherences (c) across subjects.

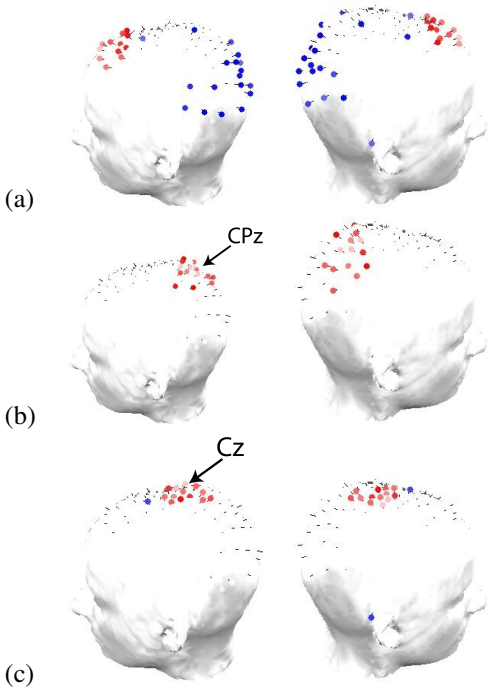

Figure 2: Topographical overviews of the most significant electrodes for the (a) eye blink, (b) stimulus and (c) response regressors. Red and blue reflect positive and negative weights, respectively, and the shading indicates the magnitude of the weights.

tion coherence was set such that they performed at roughly 70 and 90% correct (Figure (c)). These results are consistent with a DDM parametrization in which thresholds are roughly constant and the rate of evidence accumulation is high for the high coherence condition, and low for the low coherence condition.

Before running the GLM on the ramp regressors, we verified our method by plotting the main loadings of the eye blink, stimulus and response regressors. Figure 2 shows that as expected, eyeblinks have a frontopolar topography, whereas stimulus and response regressors (which were generated based on electrodes Cz and CPz, respectively) have a more central distribution centered around their respective generator electrode.

Having established that the GLM[3] is a viable method to analyze EEG data, we used canonical correlation (CC), a multivariate technique, to search for the hypothesized ramp dynamics in our data. The advantage of CC is that it allows linear combinations of channels to predict linear combinations of regressors. Because it is more difficult to interpret linear combinations of regressors, we initially restricted our attention to single regressors. Nevertheless, preliminary data indicate that ±40% larger CCs can be obtained by allowing linear combinations of regressors.

To be able to do group analysis, we had to take a subset of the data for every participant to further reduce computational load. We then performed a CC between the regressors and the EEG time series for every channel, and at every frequency. We did a separate CC for every frequency band, because we sought to make inferences about which would show most evidence of ramping activity.

One may wonder whether a CC based on a subset of each subject's data is valid. To address this concern, we compared the correlation value of the canonical correlate of interest with the predicted correlations within each subject (i.e., using the complete data for each subject). Figure 3 shows that the within-subject correlations based on a subject's complete

[3]Which predicts the time series of a single electrode by a linear combination of regressors.

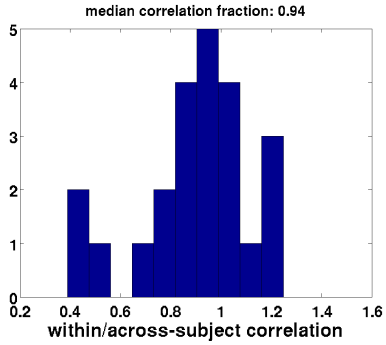

Figure 3: Validation of the subset method: within-subject correlation of weighted regressors with EEG data divided by the across-subject CCs. A perfect validity of the subset method would yield a fraction of one (within-subject correlations equal to across-subject CC).

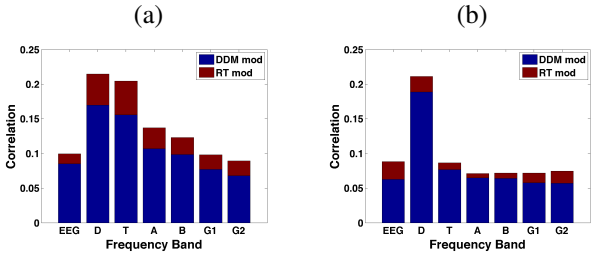

Figure 4: CC as a function of frequency, with the DDM-modulated model in blue and additional correlation achieved by the RT-modulated model in red, shown separately for the ramp regressor of (a) dots and (b) arrows.

data, weighted by the coefficients obtained from the CC, have very similar correlations to the across-subject CC based on a subset of a subject's data [sign-test comparing median correlation to 1: $p = 0.21$[4]].

Figure 4(a) shows for every frequency range (as well as non-wavelet-transformed EEG) the CC of the upramp. This correlation is largest in the 2–4 Hz delta and 4–9 Hz theta bands. The CC in the theta band is specific to the dots condition, whereas the CC in the delta band occurs also for the non-integration (arrows) condition (Figure 4(b)). This suggests that theta oscillations are a more likely candidate for a neural correlate of evidence accumulation than delta oscillations. The downramp and boxcar regressors show a much lower correlation [in the theta band the CCs are 0.11 for the boxcar, 0.076 for downramp dots, and 0.15 for downramp arrows]. All CCs have highly significant p-values because of the large number of datapoints [all ps < 0.001].

We then asked to what extent the DDM, free from trial-to-trial variations in RT, could predict the same EEG data. To do this, we compared the CCs for a regressor that was ramping up or down exactly in concordance with RT to that of a regressor that was more stereotyped: it had a fixed length (time-locked to the response) but was modulated by an individual's DDM parameters.[5] Because the DDM-modulated regressor is not yoked to RT, it fails to capture the stochastic noise in RT. Although as would be expected, the CCs are uniformly heigher for the RT-based regressor than for the DDM-modulated regressor, it is remarkable that the DDM explains a large fraction from the variance that the RT-yoked regressor can. In other words, the model is able to account for a large portion of the neural variance in ramp-like behavior.

Table 1: Mean (sem) DDM parameters for best-fitting model, separately for low and high coherence (integration condition), and arrows (non-integration conditions). cond: condition. T0: non-decision time. z: starting point. Model fits were obtained from the DMA toolbox (VandeKerckhove & Tuerlinckx, 2008)

cond	drift	threshold	T0	z
low	0.060 (0.0041)	0.157 (0.008)	0.428 (0.012)	0.078 (0.0042)
high	0.162 (0.0132)	0.147 (0.009)	0.421 (0.020)	0.078 (0.0042)
arrows	0.784 (0.069)	0.210 (0.036)	0.219 (0.009)	0.094 (0.027)

Figure 5 shows the time courses of the canonical correlate in the theta band that has the heighest (negative) weight on the dots upramp regressor. The time course of the ramp regressor is much larger for the integration condition (green) than for the arrow trials, the non-integration condition (magenta). The discontinuities close to the stimulus and response are caused by the subtraction of the nuisance regressors.

[4]Of course one should keep in mind that it's impossible to prove the null hypothesis

[5]Regressor height was modulated by the threshold parameter; its slope by the drift parameter and the ramp onset was delayed by the non-decision time.

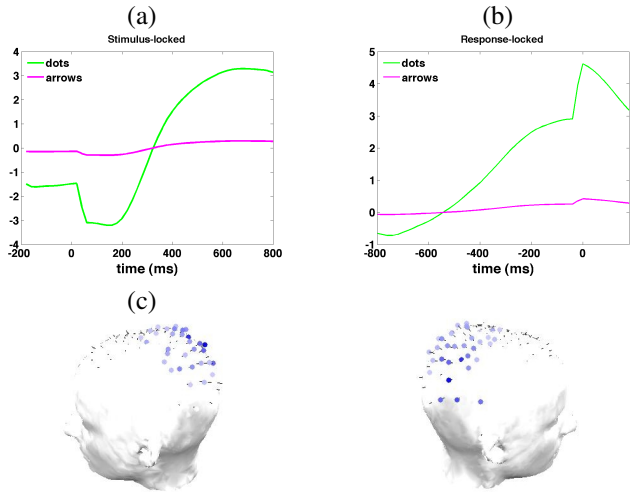

Figure 5: Stimulus-locked (a) and response-locked (b) time courses of the canonical correlate in the 4–9 Hz theta band, correlating with the dots upramp, and (c) its topography (blue indicates a negative correlation between oscillatory power and the regressor). The shade of the color indicates the magnitude of the correlation.

We next asked whether the dynamics of this ramp covaried with individual differences in DDM parameters. Table 1 shows the mean DDM fits across subjects. The mean (sem) Maximum Likelihood fit value across subjects was 3466 (167) and the mean BIC (Bayesian Information Criterion) was 3508 (167). We found a significant correlation [$r(22) = 0.36$, $p = 0.019$] between an individual's drift rate and the slope of the average theta-band time course for that same person. There was no significant correlation between the level the time course reached at the end of the response interval and the threshold [$r(22) = -0.11$, $n.s.$].

If our putative neural ramp correlate indeed reflects the drift rate, then it should be possible to divide trials into those with a short and long RT based on the thus-defined neural drift rate. Figure 6 shows that this can indeed be done for a subset of the participants (four examples are given). Subsequent fits of the DDM on the subsets of trials for these participants verified that higher neural drift was associated with a higher behavioral drift (Figure 7). The fact that this is not possible for all participants might be related to (1) problems with their EEG data quality or (2) non-optimal task performance where participants engage in different cognitive processes (distraction) in a large fraction of the trials. A further investigation of this is left for later work.

Discussion

We have confirmed our hypothesis that 4–9 Hz theta oscillations exhibit dynamics consistent with evidence accumulation in a perceptual decision making task more so than oscillations at other frequencies. In addition, the magnitude of the difference between the slopes of these potential "neural accumulators" covaries with individual differences in the drift rates

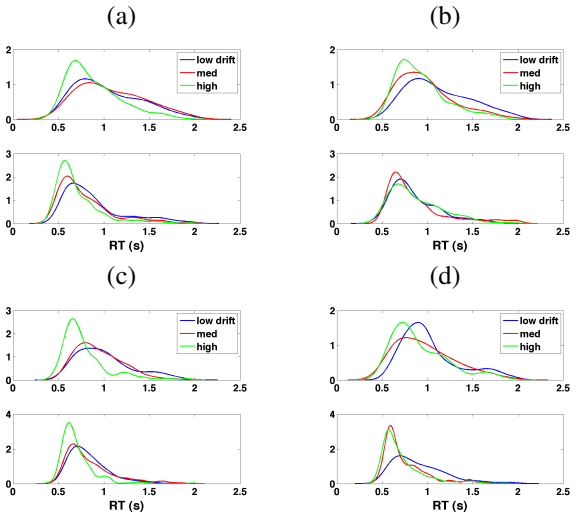

Figure 6: Neural estimates of the drift rate (binned in tertiles), based on the slope in the period of 500–100 ms before the response, can be used to predict RT bins (slow, medium, fast). Four examples of participants are shown, with the top row of each panel reflecting low coherence and the bottom row high coherence.

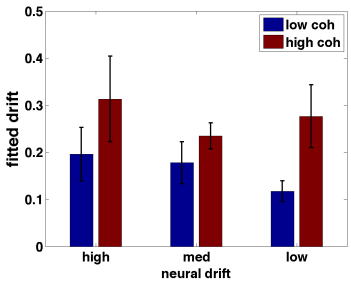

Figure 7: Fits of the DDM drift rate parameter to trials that were grouped based on the neural drift (slope 500–100 ms pre-response).

obtained from the behavioral data.

These results support previous findings of the involvement of theta oscillations in decision making (e.g., Cavanagh et al., 2010; Jacobs et al., 2006). Although the ramp regressor also loads fairly strongly on activity in the delta range, this frequency also shows a significant correlation with activity in the non-integration control task. This suggests that while theta may be specific to evidence accumulation, delta may reflect a more generic "on-task" process. The fairly large loading on the alpha regressor may reflect bleeding-in of theta activity because there are individual differences in the ranges of alpha and theta oscillations (Klimesch, Schirnke, & Pfurtscheller, 1993). One may wonder what is particular about the theta frequency that would make it suitable for a function in decision making. A modeling study by Smerieri, Rolls, and Feng (2010) suggests a possible answer. They showed that in simulated spiking neural networks of two populations of mutually-inhibiting neurons, RTs decreased and drift rates increased with increasing theta power. This effect was specific to the theta range because higher frequencies are too fast to modulate the cell's membrane potential, which acts as a low-pass filter.

What is quite surprising in our neural correlate of evidence accumulation is that instead of it increasing, oscillatory power actually decreases over the course of the decision interval. It may be that decreases in oscillatory power actually reflect increases in functional brain activity. This is consistent with Lorist et al. (2009), who found that oscillatory power increases with fatigue, implying it increases with productive task performance. It may also be the case that over the course of evidence accumulation, one moves from a more global mode of processing, in which information is combined from a large number of neurons, to combining information from a much smaller set of neurons (associated with less synchronization and lower oscillatory power). Both of these hypotheses could be tested with more localized neural recordings obtained from e.g., intracranial EEG. A third possibility is that theta may reflect the amount of uncertainty rather than the evidence accumulation process per se.

One may also wonder why the correlations between the neural accumulators and EEG data, although significant, are fairly low. In fact, the order of magnitude of correlations that we obtained are not unlike those obtained in GLMs applied to fMRI data. This is caused by the large amount of noise in neural data. Future studies should investigate whether this can be improved by applying e.g., independent component analysis (Delorme, Makeig, & Sejnowski, 2001). Also regularization, which focuses on the informative features in the data, could possibly help to increase the correlation between model dynamics and EEG data.

Our findings have several implications for future research. First, the correlates of the DDM that are observable in EEG can be used to assess the effect of task manipulations (such as speed-accuracy trade-off or reward rate) on accumulation dynamics. Second, there are large individual differences in task performance. EEG signatures of neural accumulators may allow us to distinguish different types of participants or strategies, given that individual differences in DDM parameters covaried with the slope of the neural accumulation signal. The "neural accumulators" thereby soak up some portion of the noise in the model. These "neural accumulators" may also capture individual trial noise, such as attentional fluctuations, although that remains to be proven. Third, we can use the same multivariate methods to clarify the topographical location of possible neural accumulators in fMRI data. Finally, it is important to consider what implications our results have for models of decision making. For example, the non-linearity of the accumulator time courses suggests that evidence accumulation may better be described by a competitive evidence integration than by a linear ballistic accumulator (Brown & Heathcote, 2008). Yet, it is difficult to distinguish between the remaining accumulator mod-

els based solely on their dynamics in two-alternative forced choice tasks (Ditterich, 2010).

In short, we have provided evidence for a neural correlate of the dynamics of evidence accumulation in decision making measured in human EEG. Accumulation dynamics were captured best by 4–9 Hz theta oscillations in a set of superior parietal channels, and covaried with individual differences in DDM parameters.

Acknowledgments

The authors gratefully acknowledge funding from the AFOSR Multi-University Research Initiative FA9550-07-1-0537, and Conte Center MH062196 grants. They also like to thank Valerie Karuzis, Jillian Brinberg, Peter Foster, Laura deSouza, and Brian Schilder for help with testing participants.

References

Brainard, D. H. (1997). The psychophysics toolbox. *Spatial Vision*, *10*, 443-446.

Britten, K. H., Shadlen, M. N., Newsome, W. T., & Movshon, J. A. (1992). The analysis of visual motion: a comparison of neuronal and psychophysical performance. *Journal of Neuroscience*, *12*(12), 4745–4765.

Brown, S. D., & Heathcote, A. (2008). The simplest complete model of choice reaction time: Linear ballistic accumulation. *Cognitive Psychology*, *57*, 153–178.

Busch, N. A., & VanRullen, R. (2010). Spontaneous eeg oscillations reveal periodic sampling of visual attention. *Proc. Nat. Acad. Sci., USA*, *107*(37), 16048–16053.

Cavanagh, F., James, Frank, M. J., Klein, T. J., & Allen, J. J. B. (2010). Frontal theta links prediction errors to behavioral adaptation in reinforcement learning. *NeuroImage*, *49*, 3198–3209.

Delorme, A., Makeig, S., & Sejnowski, T. (2001, December). Automatic artifact rejection for EEG data using high-order statistics and independent component analysis. In *Proceedings of the Third International ICA Conference.* San Diego.

Ditterich, J. (2010). A comparison between mechanisms of multi-alternative perceptual decision making: ability to explain human behavior, predictions for neurophysiology, and relationship with decision theory. *Frontiers in Neuroscience*, *4*, 184.

Friederici, A. D., Wang, Y., Herrmann, C. S., Maess, B., & Oertel, U. (2000). Localization of early syntactic processes in frontal and temporal cortical areas: a magnetoencephalographic study. *Human Brain Mapping*, *11*(1), 1–11.

Fries, P. (2009). Neuronal Gamma-band Synchronization as a Fundamental Process in Cortical Computation. *Annual Review of Neuroscience*, *32*(1).

Fries, P., Nikolić, D., & Singer, W. (2007). The gamma cycle. *Trends in Neurosciences*, *30*(7), 309–316.

Gold, J. I., & Shadlen, M. N. (2001). Neural computations that underlie decisions about sensory stimuli. *Trends in Cognitive Science*, *5*(1), 10–16.

Hestvik, A., Maxfield, N., Schwartz, R. G., & Shafer, V. (2007). Brain responses to filled gaps. *Brain and Language*, *100*(3), 301–316.

Jacobs, J., Hwang, G., Curran, T., & Kahana, M. J. (2006). EEG oscillations and recognition memory: Theta correlates of memory retrieval and decision making. *NeuroImage*, *15*(2), 978–87.

Kahana, M. J., Seelig, D., & Madsen, J. R. (2001). Theta returns. *Current Opinion in Neurobiology*, *11*, 739–744.

Klimesch, W., Schirnke, H., & Pfurtscheller, G. (1993). Alpha frequency, cognitive load and memory performance. *Brain Topography*, *5*(3), 241–251.

Lorist, M. M., Bezdan, E., ten Caat, M., Span, M. M., Roerdink, J. B. T. M., & Maurits, N. M. (2009). The influence of mental fatigue and motivation on neural network dynamics; an EEG coherence study. *Brain Research*, *1270*, 95–106.

O'Keefe, J., & Burgess, N. (1999). Theta activity, virtual navigation and the human hippocampus. *Trends Cogn Sci*, *3*(11), 403-406.

O'Keefe, J., & Recce, M. L. (1993). Phase relationship between hippocampal place units and the EEG theta rhythm. *Hippocampus*, *3*, 317–30.

Ratcliff, R. (1978). A theory of memory retrieval. *Psychological Review*, *85*, 59-108.

Shadlen, M. N., & Newsome, W. T. (2001). Neural basis of a perceptual decision in the parietal cortex (area LIP) of the rhesus monkey. *Journal of Neurophysiology*, *86*(4), 1916–1936.

Smerieri, A., Rolls, E. T., & Feng, J. (2010). Decision time, slow inhibition, and theta rhythm. *Journal of Neuroscience*, *30*(42), 14173–14181.

Tabachnick, B. G., & Fidell, L. S. (2005). *Using multivariate statistics*. Pearson Education.

van Vugt, M. K., Sekuler, R., Wilson, H. R., & Kahana, M. J. (in revision). Distinct electrophysiological correlates of proactive and similarity-based interference in visual working memory.

VandeKerckhove, J. A., & Tuerlinckx, F. (2008). Diffusion model analysis with MATLAB:A DMAT primer. *Behavior Research Methods*, *40*(1), 61–72.

Womelsdorf, T., Schoffelen, J., Oostenveld, R., Singer, W., Desimone, R., Engel, A., et al. (2007). Modulation of Neuronal Interactions Through Neuronal Synchronization. *Science*, *316*(5831), 1609.

Womelsdorf, T., Vinck, M., Leung, L. S., & Everling, S. (2010). Selective theta-synchronization of choice-relevant information subserves goal-directed behavior. *Frontiers in Human Neuroscience*, *4*, 210.